

# **NICKEL-COBALT-SULFIDE FOR SUPERCAPACITOR APPLICATIONS**

A Project Report Submitted as part of concern for the degree of

**MASTER OF SCIENCE**

By

**ISHITA NASKAR**

(Roll No: - CY17MSCST11008)

Under the guidance of

**Dr. M. DEEPA**



भारतीय प्रौद्योगिकी संस्थान हैदराबाद  
Indian Institute of Technology Hyderabad

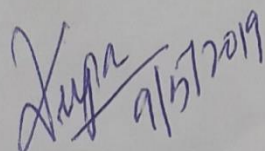
**DEPARTMENT OF CHEMISTRY**

**INDIAN INSTITUTE OF TECHNOLOGY  
HYDERABAD, INDIA**

## Declaration

I hereby declare that the matter embodied in this report is the result of investigation carried out by me in the Department of Chemistry, Indian Institute of Technology Hyderabad under the supervision of **Dr. M. Deepa**

In keeping with general practice of reporting scientific observations, due acknowledgement has been made wherever the work described is based on the findings of other investigators.

  
9/5/2019

Signature of the Supervisor

Dr. M. Deepa  
Head & Professor  
Department of Chemistry  
Indian Institute of Technology Hyderabad  
Kandi-502285, Sangareddy, Telangana, India

ISHITA NASKAR

(Signature)

Ishita Naskar

(Student Name)

CY17MSCST11008

(Roll No)

Approval Sheet

This thesis entitled as "Nickel-Cobalt-Sulfide for Supercapacitor Applications" acknowledged by Ishita Naskar is approved for the degree of Master of Science from Indian Institute of Technology, Hyderabad.



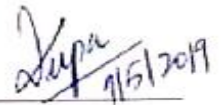
Name and affiliation

Examiner



Name and Affiliation

Examiner



Name and affiliation

Dr. M. Deepa

Head & Professor

Department of Chemistry, Advisor

Indian Institute of Technology Hyderabad

Kandi-502335, Sangareddy, Telangana, India

Scanned by CamScanner

# ACKNOWLEDGEMENT

Above all I am very much grateful to God because of completion of this project with successfulness. After this I am very much obliged to my supervisor **Dr. M. Deepa** for giving me the precious opportunity to start this project and in addition to this, for her encouragement and guidance throughout the tenure of my project and moreover for her constant support. I would like to thank her also for helping me to complete it smoothly.

I would like to thank Ph.D. scholar **Mr. Manoranjan Ojha** for his constant help and support and Mr. Sathish Deshangani for his advice. I am also grateful to my other lab mates for their helpful thoughts in my Project work.

I am deeply grateful to my Head of Department, Dr. M. Deepa, and to the entire Department of Chemistry, IIT Hyderabad, for extending all necessary facilities for the completion of this project.

My deep appreciation goes to my beloved parents Mr. Nemaï Chandra Naskar and Mrs. Sonali Naskar for supporting me throughout my life.

# ABSTRACT

Nickel-cobalt-sulfide has been the highly probable electrocapacitive components for storing energy in electrical equipments, because of their maximum electrical conductivity and various and different oxidation states. Ni-Co-S crystals is synthesized by the hydrothermal method. Cyclic voltammetry, galvanostatic charge discharge, and electrochemical impedance spectroscopy (EIS) had been used to study the different electrochemical properties of Nickel-Cobalt-Sulfide, Carbon and Nickel-Cobalt-Sulfide@Carbon cloth structures. Electrochemical properties of Ni-Co-S, Ni-Co-S@Carbon cloth as supercapacitor electrodes were examined in 3 Molar Potassium Hydroxide electrolyte. The maximum Specific Capacitance of Nickel-Cobalt-Sulfide, Carbon and Nickel-Cobalt-Sulfide@Carbon cloth are  $4000 \text{ F g}^{-1}$ ,  $4200 \text{ F g}^{-1}$  at  $5 \text{ A g}^{-1}$  and  $1400 \text{ F g}^{-1}$  at  $1 \text{ A g}^{-1}$  respectively. High energy densities of Nickel-Cobalt-Sulfide, Carbon and Ni-Co-S@Carbon cloth are  $560 \text{ Wh Kg}^{-1}$ ,  $580 \text{ Wh Kg}^{-1}$  and  $190 \text{ Wh Kg}^{-1}$  respectively. Highest Power Density of Nickel-Cobalt-Sulfide, Carbon and Nickel-Cobalt-Sulfide@Carbon cloth have been  $12500 \text{ W Kg}^{-1}$ ,  $8450 \text{ W Kg}^{-1}$  and  $5000 \text{ W Kg}^{-1}$  respectively. These results demonstrate that the developed nickel-cobalt-sulfide crystals have encouraging utilizations in electrochemical supercapacitors

# CONTENTS

<i>Declaration</i> .....	
<i>Approval Sheet</i> .....	
<i>Acknowledgement</i> .....	
<i>Abstract</i> .....	
<i>Contents</i> .....	
<i>List of table</i> .....	

## **Chapter 1. Introduction 9-20**

<i>1.1 Historical Background</i>	
<i>1.2 Capacitors</i> . . . . .	
<i>1.3 Supercapacitors</i> . . . . .	
• <i>Electric double-layer capacitors</i> . . . . .	
• <i>Pseudo capacitors</i> . . . . .	
• <i>Hybrid supercapacitors</i>	
<i>1.4 Contrast between the energy and power densities of supercapacitors, capacitors batteries and fuel cells</i>	

## **Chapter 2. Supercapacitor Electrochemical Characterization Techniques 21-27**

<i>2.1 Cyclic Voltammetry</i>	
<i>2.2 Galvanostatic Charge and Discharge</i>	
<i>2.3 Electrochemical Impedance Spectroscopy</i>	
<i>2.4 Energy and Power density</i>	
<i>2.5 Summary of Literature Survey</i>	

## **Chapter 3. Experimental Section (a) 28-39**

<i>3.1 Chemicals</i>	
<i>3.2 Preparation of sample (Synthesis of Ni-Co-S)</i>	
<i>3.3 Preparation of Carbon from puffed rice</i> .....	
<i>3.4 Fabrication of cells</i>	
<i>3.5 Result and discussion</i>	
<i>3.5.1 Electrochemical properties</i>	

## Chapter 4.

**Comparison among the CVs of Nickel-Cobalt-Sulfide, Carbon and Nickel-Cobalt-Sulfide electrodes** **40**

**Conclusion.....41**

**References.....42-46**

### List of figures:

1. 1.2a) Schematic diagram of capacitor.
2. 1.2b) Schematic Symbol of the Capacitor.
3. 1.2c) Circuit presentation of a capacitor.
4. 1.3A) Components of a Supercapacitor.
5. 1.3B) Types of Supercapacitors.
6. 1.3C) Charging of a Supercapacitor
7. 1.3D) Discharging of a supercapacitor
8. 1.3.1a) Structure of EDLC.
9. 1.3.1b) Charge and Discharge of EDLC
10. 1.3.2a) Components of a Pseudocapacitance
11. 1.4) Ragone Plot of energy storage devices
12. 2.1) A schematic view of cyclic voltammogram
13. 2.2) Galvanostatic Charge-Discharge
14. 2.3) Nyquist plots of Nickel-Metal-Organic-Framework and Nickel/Cobalt-Metal-Organic-Framework-5, and the equivalent circuit of Ni/Co-MOF-5 (inset).
15. 2.4) Ragone plots of the Cobalt-Nickel-Sulfide//AC hybrid capacitor
16. 3.5.1a) Cyclic Voltammetry curves of Nickel-Cobalt-Sulfide measured at the variety of scanning rates from  $5 \text{ mVs}^{-1}$  to  $25 \text{ mVs}^{-1}$  in a  $3\text{M KOH}$  electrolyte
17. 3.5.1b) Galvanostatic charge/discharge curves of Nickel-Cobalt-Sulfide low and high current density of Ni-Co-S are from  $5 \text{ A g}^{-1}$  to  $10 \text{ A/cm}^2$ .
18. 3.5.1c) Dependences of specific capacitance of Nickel-Cobalt-Sulfide at diversified current densities from  $5 \text{ A g}^{-1}$  to  $10 \text{ A g}^{-1}$  for charge-discharge behavior.

19. 3.5.1d) Nyquist plot for Ni-Co-S, obtained in 3M KOH electrolyte at frequency range 0.1 Hz to 1 MHz
20. 3.5.1e) Comparison of energy and power densities of Ni-Co-S/Carbon cloth SCs in a Ragone plot.
21. 3.5.2a) CV curves of Carbon measured at the various scan rates from  $1\text{ mVs}^{-1}$  to  $25\text{ mVs}^{-1}$  in a 3M KOH electrolyte,
22. 3.5.2b) Galvanostatic charge/discharge curves of Carbon low and high current density of Carbon are from  $5\text{ A g}^{-1}$  to  $10\text{ A g}^{-1}$ .
23. 3.5.2c) Dependences of specific capacitance of Carbon at diversified current densities from  $5\text{ A g}^{-1}$  to  $10\text{ A g}^{-1}$  for charge-discharge behavior.
24. 3.5.2d) Nyquist plot for Carbon, obtained in 3M KOH electrolyte at frequency range 0.1 Hz to 1 MHz
25. 3.5.2e) Comparison of energy and power densities of Carbon (from puffed rice)/Carbon cloth SCs in a Ragone plot.
26. 3.5.3a) CV curves of Cell measured at the variety of scanning rates at 1, 2, 5, 10, 15, 20,  $25\text{ mVs}^{-1}$  in a 3M KOH electrolyte,
27. 3.5.3b) Galvanostatic charge/discharge curves of Cell low and high current density of Cell are from  $1\text{ A g}^{-1}$  to  $10\text{ A g}^{-1}$ .
28. 3.5.3c) Dependences of specific capacitance of Cell at variety of current densities from  $1\text{ A g}^{-1}$  to  $10\text{ A g}^{-1}$  for charge-discharge behaviour.
29. 3.5.3d) Nyquist plot for Cell, obtained in 3M KOH electrolyte at frequency range 0.1 Hz to 1 MHz
30. 3.5.3e) Comparison of energy and power densities of Cell in a Ragone plot.

#### **List of tables:**

*Table 1: Charging and Discharging of a capacitor*

*Table 2: Capacitor Vs Supercapacitor*

*Table 3: Brief description of charge discharge, specific capacitance, energy density and power density of Ni-Co-S.*

*Table 4: Brief description of charge discharge, specific capacitance, energy density and power density of Carbon*



*Table 5: Brief description of charge discharge, specific capacitance, energy density and power density of Ni-Co-S/Carbon*

## **Chapter 1. Introduction**

### **1.1: Historical Background**

The concept of supercapacitors had been in discussion since the 19th century, current technologies are finally accomplishing the leading energy storage. The General Electric engineers started their experiment with porous carbon electrodes, for designing capacitors.

The first electrochemical capacitor equipment was invented by General Electric's H.I. Becker in 1957. The person designed a low voltage electrolytic capacitor which had absorbtive carbon electrodes, assuming that the energy can be reserved as a charge in the carbon pores. Becker was granted the first patent on supercapacitor at General Electric Corp. He utilized the porous carbon material with the high surface area to propose a capacitor. But he was unaware of the double layer mechanism.

Subsequent, in 1966 scientists of Standard Oil of Ohio developed another electrical energy storage setup. Their invention was not commercialized, licensing the technology to Nippon Electric Corporation in 1971. Their supercapacitor trademarked product of 5cm<sup>3</sup> size was rated at 5.5V and had capacitance upto the value of 1F.

During the period of 1975 to 1980, significant works were done by Brian Evans Conway. At the end of 1980s, electrode materials were upgraded to give good and increased capacitance values. Electrolytes were also developed.

In 1982, the 1<sup>st</sup> supercapacitor with low internal resistance was developed.

In 1991, Brian Evans Conway differentiated between a Battery and a Supercapacitor.

### **1.2: CAPACITOR**

A capacitor is a cell which stores and releases electrical energy in the form of charge.

A capacitor contains the following:

- two conductors between which there is a section which does not conduct heat or electricity. This non-conducting region can either be a vacuum or an electrical insulator component, designated as a dielectric.
- Examples of dielectric media are glass, air, paper, plastic, ceramic, and even a semiconductor deficient region chemically indistinguishable to those who can conduct heat and electricity.

The capacitor was formerly designated as a condenser or condensator.

Capacitance( $C$ ) is designated as the electrical charge over each conductor divided by the potential difference between them. The unit of capacitance in the International System of Units (SI) is the farad (F), defined as one coulomb per volt (1 C/V).

$$C = Q/V$$

Where  $Q$  represents the charge and  $V$  denotes the voltage.

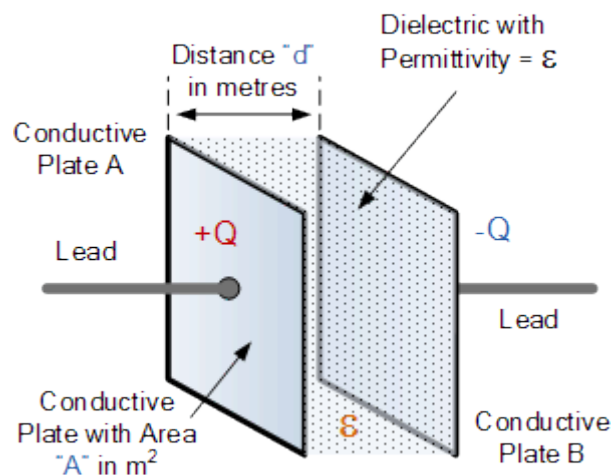


**Fig. 1.2a: Schematic diagram of capacitor**

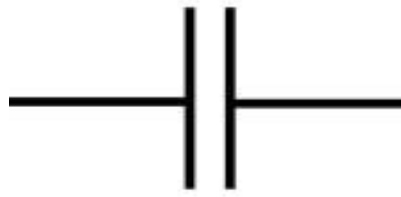


**Fig. 1.2b: Schematic Symbol of a Capacitor**

**Table 1: Charging and Discharging of a capacitor**

Charging a Capacitor	Discharging a Capacitor
<ul style="list-style-type: none"> <li>• It is connected to a DC power supply with current flowing through the circuit.</li> <li>• Both plates get equal and opposite charges</li> <li>• Potential difference is created.</li> <li>• Terminal voltage(<math>V_C</math>) = Supplied Voltage(<math>V</math>), implying that capacitor is fully charged.</li> </ul>	<ul style="list-style-type: none"> <li>• Capacitor is disconnected from the power supply</li> <li>• It discharges through Resistor</li> <li>• Voltage between plates drops down to 0 V.</li> </ul>

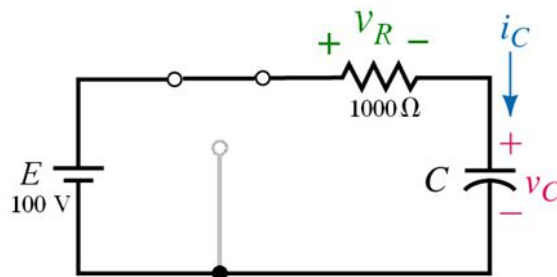


**Fig. 1.2c: Circuit presentation of a capacitor**

### **Applications of Capacitors:**

- They are used in many electronic devices and electrical systems
- It can be used as a temporary battery, since it can store energy while connected to charging circuits and can dissipate the energy when disconnected.
- They are mainly used in consumer electronics and automotive vehicles.

### **1.3: SUPERCAPACITOR**

Supercapacitor have been again designated as double-layer capacitors or ultracapacitors. As a substitute for the regular dielectric, supercapacitors utilize two systems for storing electrical energy:

- Double-layer capacitance: electrostatic in origin, while
- Pseudocapacitance is electrochemical, which designates that supercapacitors couple the functionings of ordinary capacitors with the functionings of an ordinary battery. One attractive function has been the storing of energy in KERS, or dynamic-braking systems (Kinetic Energy Recovery System) in

automotive industry.

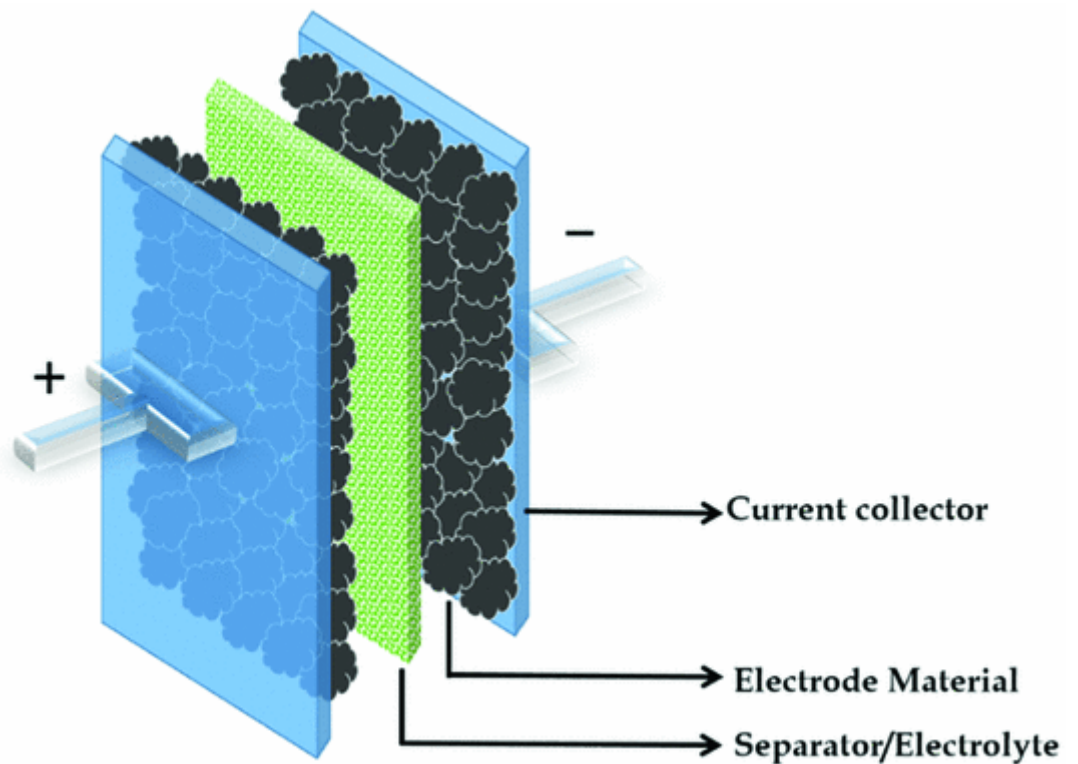


**Fig. 1.3A: Components of a Supercapacitor.**

**Reference:**

Q Abbas, Pajak D. Pajak, E. Frackowiak, F. Beguin, *Electrochim Acta* ,**140**, 132.

For the reason of storing electrical charge, a supercapacitor utilizes porous materials in the form of separators so that they can accumulate ions in those orifices at an atomic level. The most regularly utilized component of modernized supercapacitors is activated charcoal. For the fact that carbon is incapable of being a good insulator, so the consequence is an enormous functioning voltage limited to only 3 V. Activated charcoal has one disadvantage: the charge carriers are indistinguishable in parameter to the orifices in the material and some of them are incapable of fitting into the smaller pores, the consequence is the reduced storage capacity. Supercapacitors have also some of the disadvantages as well. One of the most probable disadvantage is a relatively low specific energy. The specific energy is designated as the total quantity of energy stored in the electrical equipments which is divided by its weight.

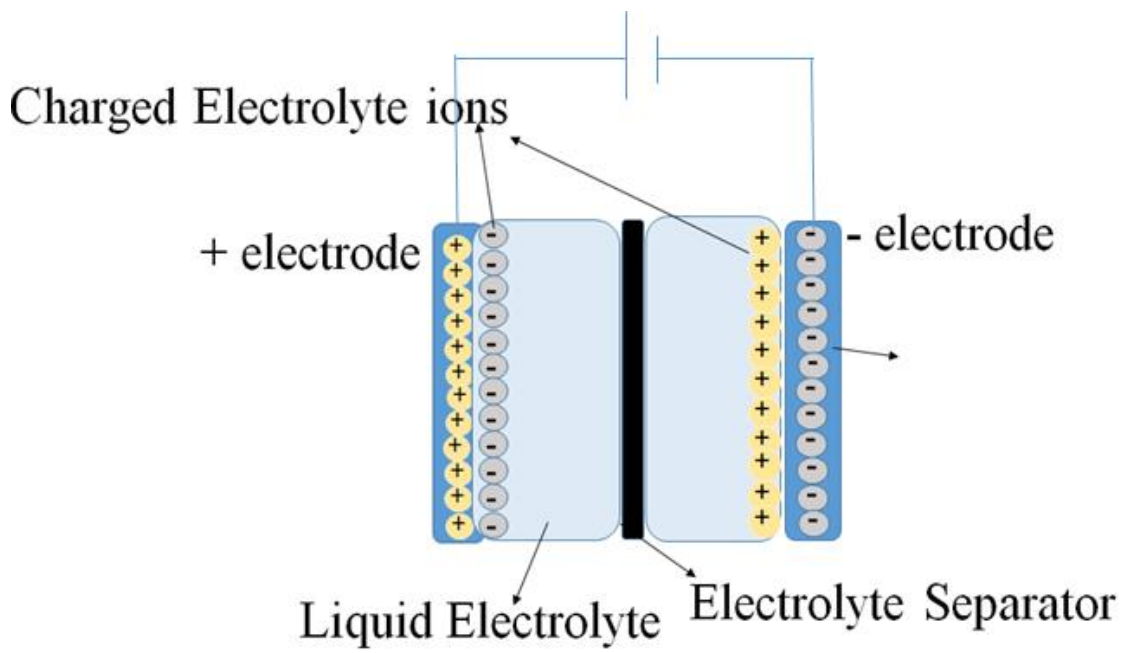


**Fig. 1.3B: Charging of a Supercapacitor**

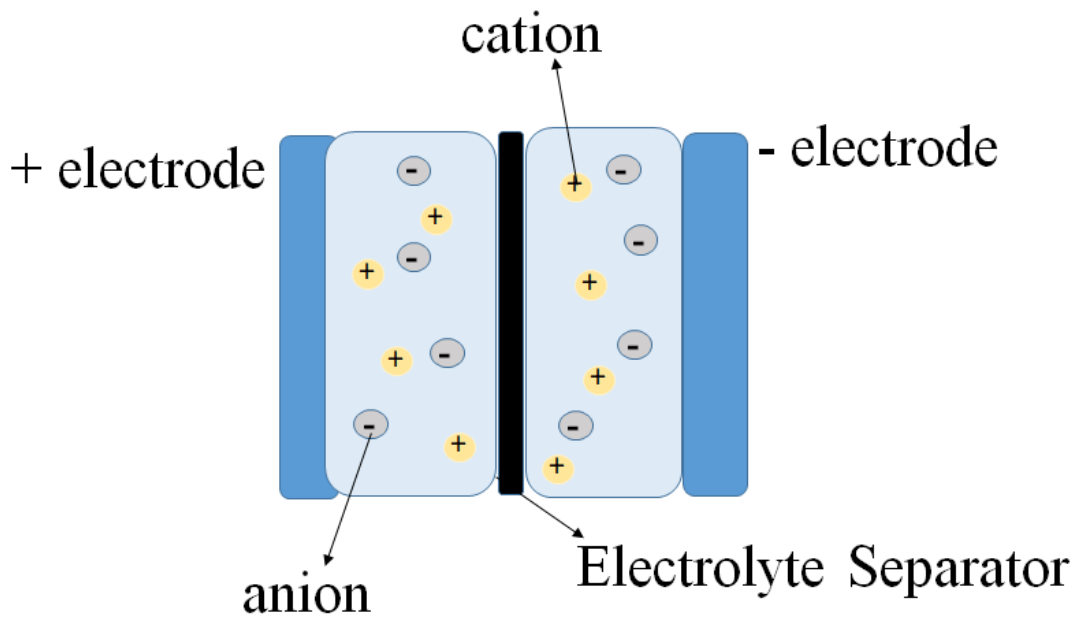


**Fig. 1.3C: Discharging of a Supercapacitor**

**Table 2: Capacitor Vs Supercapacitor**

CAPACITOR	SUPERCAPACITOR
1. Low Energy density	1. High energy density
2. Low capacity	2. High capacity
3. Low power density	3. High power density
4. Stores electrical charge and capable of discharging	4. Can be charged and discharged continuously.
5. Dielectric material : ceramic, aluminium oxide	5. Activated carbon is used as both electrodes and an electrolyte separates the two electrodes.
6. Cheap	6. Expensive

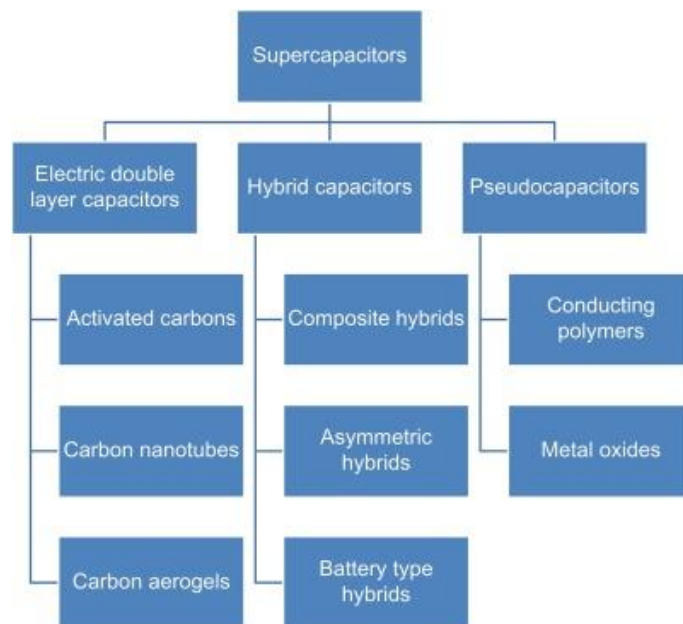


**Fig. 1.3D: Types of Supercapacitors**

**Reference:**

R. S. Kate, S. A. Khalate & R. J. Deokate, *J. Alloys Compd.*, 2018, **734**, 89



### **1.3.1) Electrostatic double-layer capacitors (EDLCs)**

Electric Double Layer Capacitors (EDLC)s also designated as Ultracapacitors, or Supercapacitors are rechargeable substitute for storing energy in electrical devices. The Electric Double Layer Capacitors are mainly used with a battery but in some cases the real option is to supplant the battery. EDLCs are an excellent source of back-up and peak-power.

Electrical Double Layer Capacitor (EDLC) does not consist of any regular dielectric. Instead, an electrolyte (solid or liquid) is incorporated in the middle of the two electrodes. In EDLC, an electrical situation designated as "electrical double layer" have been assembled in the middle of the electrodes and the electrolyte functions in the form of a dielectric.

EDLCs employ an electrochemical double-layer of charge for storing energy. After applying the voltage, charges are assembled over the electrode surfaces. Following the phenomenon (opposite charges are attracted towards each other), charged particles in the electrolyte solution disperse across the separator into the orifices of the electrode of opposite charge. Consequently, a double-layer of charge is created over each electrode. These double-layers, connected with an increase in surface area and a reduction in the separation amidst the electrodes, permit the EDLCs to attain higher energy densities than traditional capacitors.

As a result of no transmission of charge in the middle of electrolyte and electrode, there are no chemical or composition changes correlated with non-Faradaic processes. As a consequence of this, storing charge in EDLCs is efficiently reversible, which makes them to achieve very high cycling stabilities. EDLCs generally function with long-lasting performance characteristics for many charge-discharge cycles, sometimes as many as  $10^6$  cycles. On the other hand, electrochemical batteries about  $10^3$  cycles. Due to their long term cycling stability and low maintenance requirements, EDLCs are very much suitable for operations that indulge non-user dependable positions, such as deep sea or mountain environments

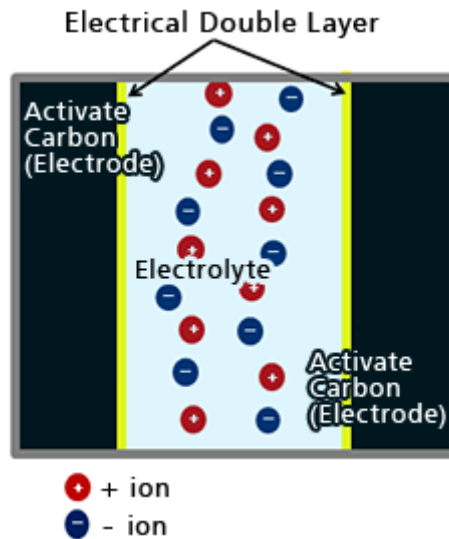


**Fig. 1.3.1a: Structure of EDLC**

The mechanistic pathway by which the charged particles are consumed and released to the electrical double layer contributes to charge and discharge of EDLCs. By application of the voltage to the facing electrodes, the charged particles get attracted to the exterior part of the electrical double layer and EDLC is charged. On the contrary, they retreat away while discharging EDLC. Thus with the help of this process, the EDLC is charged and discharged.

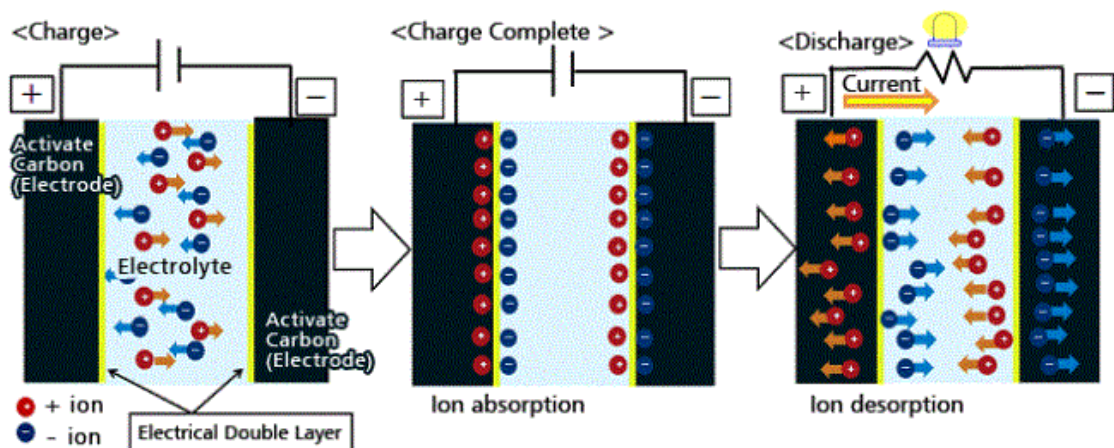


**Fig. 1.3.1b: Charge and Discharge of EDLC**

### 1.3.2) Pseudocapacitors:

- Pseudocapacitors store electrical energy in a faradaic process by electron charge transfer in the middle of electrode and electrolyte.
- This is accomplished through electrosorption, reduction-oxidation reactions and implantation mechanisms, designated as pseudocapacitance.
- A pseudocapacitor is the component of an electrochemical capacitor, and coupled together with an electric double-layer capacitor (EDLC) to produce a supercapacitor.

#### Pseudocapacitance with specifically adsorbed ions

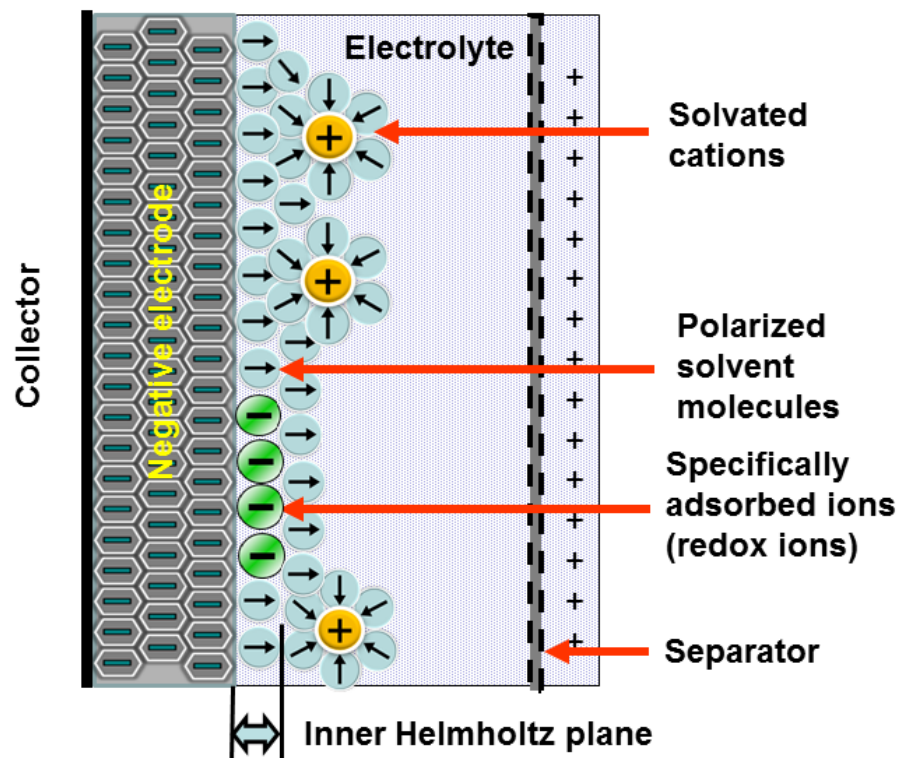


Fig. 1.3.2a: Components of a Pseudocapacitance

### **1.2c) Hybrid supercapacitors:**

Hybrid capacitors utilize the relative favourable conditions and diminish the relative drawbacks of EDLCs and pseudocapacitors to recognize excellent functioning characteristics. With the utilization of both Faradaic and non-Faradaic processes for storing charge, hybrid capacitors have attained energy and power densities greater than EDLCs without the reduction in cycling stability and affordability that have limited the benefit of pseudocapacitors.

### **1.4: Contrast between the energy and power densities of supercapacitors, capacitors batteries and fuel cells**

#### **Taxonomy of Supercapacitors**

On the basis of the current R&D trends, supercapacitors have been categorised into three familiar classes: electrochemical double-layer capacitors, pseudocapacitors, and hybrid capacitors. Each class is represented by its different mechanistic pathway in order to accumulate charge. These are, respectively, non-Faradaic, Faradaic, and a combination of the two. Faradaic processes, such as oxidation-reduction reactions, include the transmission of charge between electrode and electrolyte. A non-Faradaic mechanism, on the contrary, is incapable to utilize a chemical pathway. Rather, charges are circulated over the exterior part by physical processes that are incapable of comprising the construction or destruction of chemical bonds

A graphical classification of the variety of classes and subclasses of supercapacitors is conferred:

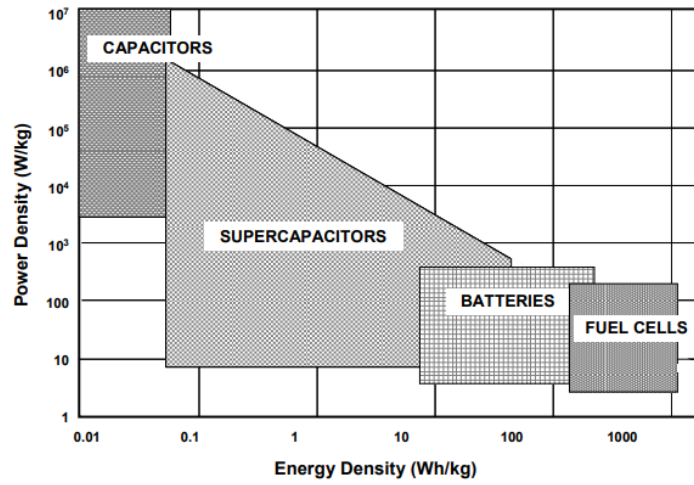


**Fig. 1.4: Ragone Plot of energy storage devices**

**Reference:**

L. Grande, V. T. Chundi, D. Wei, C. Bower, P. Andrew & T. Ryhänen, *Particuology*, 2012, **10**, 1.

## Chapter 2: Supercapacitor Electrochemical Characterization Techniques

### 2.1 Cyclic Voltammetry

Cyclic Voltammetry (CV) designates an electrochemical approach which accounts for the current which has been produced in an electrochemical cell under a sweeping bias. CV is implemented by cycling the potential of a working electrode, and evaluating the resultant current. Contradictory to the linear sweep voltammetry, after the set potential is reached in a CV experiment, the functioning electrode's potential is raised in the opposite direction to come back to the original potential. These cycles of slopes in potential may be reproduced as many times as desired.

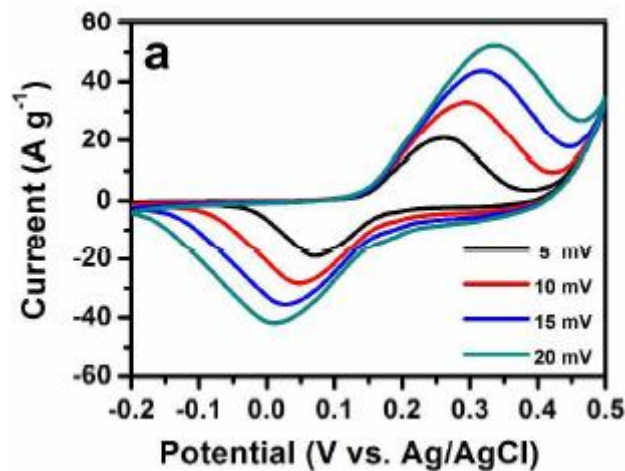


Fig. 2.1: A schematic view of cyclic voltammogram

#### References:

T. Dobbelaere, P. M. Vereecken, C. Detavernier, *HardwareX*, 2017, **2**, 34.

From the area of a CV curve, the specific capacitance of the active material is evaluated by the following equation:

$$C = \frac{1}{2} \left( \frac{\int idv}{mvU} \right)$$

Where;  $C$  designates the specific capacitance,  $m$  designates the mass of active material,  $U$  designates the potential window,  $v$  designates the scan rate, and  $\int idv$  designates the area under the CV curve. It is rational that the whole area should be divided by two to obtain the specific capacitance as a cycle comprises of both charging and discharging processes.

## 2.2: Galvanostatic Charge-Discharge

The **galvanostatic charge discharge** is a process which is another approach to calculate the electrochemical capacitance of components. A practical GCD curve is presented, in which the voltage is drawn as a function of the time. Then, one can easily regulate the specific capacitance by the potential window, current density and discharge time with the following equation:

$$C = \frac{I\Delta t}{mU}$$

where  $I$  designates the current,  $\Delta t$  designates the discharge time,  $m$  designates the mass of electrode material, and  $U$  designates the potential window.

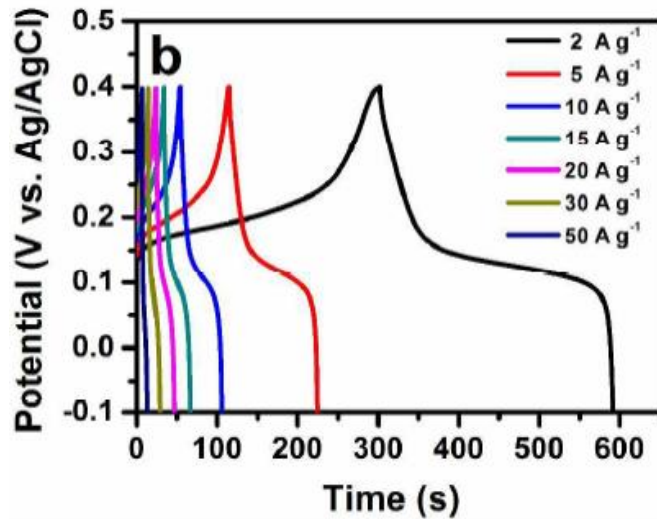


**Fig. 2.2: Galvanostatic Charge-Discharge**

**Reference:**

N. Abushrenta, X. Wu, J. Wang, J. Liu & X. Sun , *Sci. Rep.*, 2015, **5**, 1.

**2.3: Electrochemical Impedance Spectroscopy:**

In EIS, an AC voltage of fluctuating frequency is applied to the sample and a plot of impedance change vs frequency is plotted for analysis.

Besides this, Impedance is a vector quantity. So it is expressed through real and imaginary parts. It is expressed as complex impedance( $Z^*$ ).

$Z'$ ( $|Z|\cos\Theta$ ) and  $Z''$ ( $|Z|\sin\Theta$ ). This plot of  $Z'$  vs  $Z''$  is called Nyquist plot and it gives information about charge transfer and charge transport processes in the cell. A representative plot is shown below:



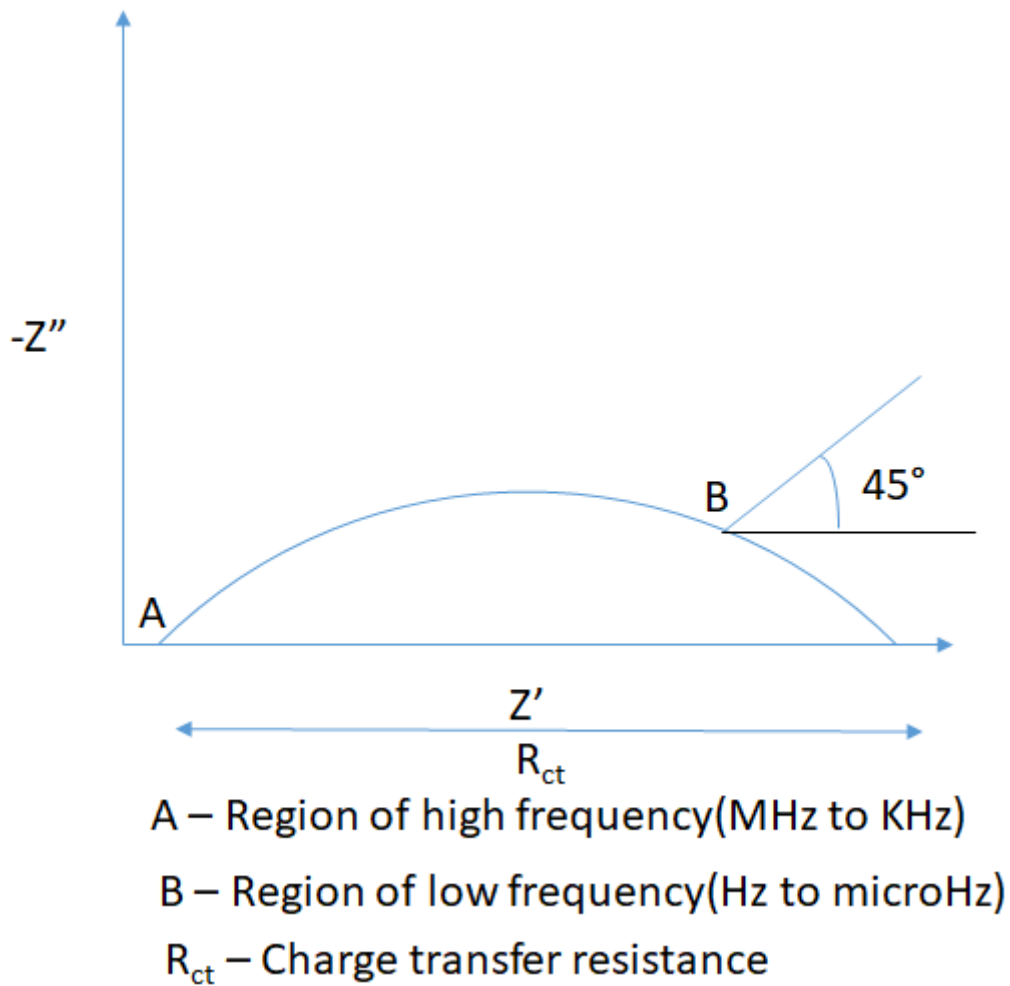


Fig. 2.3: Electrochemical Impedance

#### 2.4: Energy Density and Power Density

**Energy density** accounts for the quantity of energy stored in a given system or region of space per unit volume. Ragone plots (Fig. 9) are essential for calculating energy and power densities and are contemplated to be needful for storing energy in electrical equipments including batteries, fly wheels and ultracapacitors. The energy density has been designated as the amount of stored energy per volume in the equipment. Energy density (E) and power density (P) of the SCs could be evaluated from following:

$$E(\text{Wh/kg}) = \frac{1}{2} CV^2$$

$$P \left( \frac{W}{kg} \right) = \frac{E * 3600}{\Delta t}$$

C = Capacitance (F/g), V = Voltage (v), T = time (s)

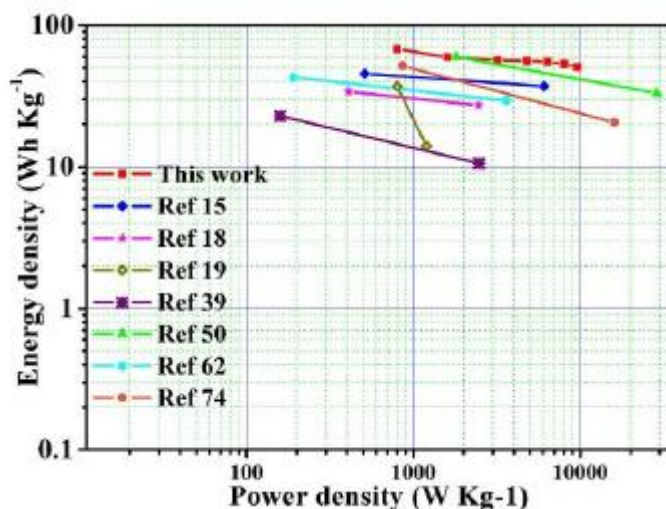


Fig. 2.4: Ragone plots of the Co-Ni-S//AC hybrid capacitor

#### Reference:

S. Rafai, C. Qiao, M. Naveed, Z. Wang, W. Younas, S. Khalid, C. Cao, *Chem. Eng. J.*, 2019, **01**, 059.

#### 2.5: Summary of Literature Survey:

In this work, pseudocapacitive and EDLC based materials were used to fabricate supercapacitors. A Ni-Co-S based chalcogenide was used as the negative electrode and an activated carbon material was used as the positive electrode. Mixed metals (such as Ni-Co) based chalcogenides are very useful because they are transition metals and they show variable oxidation states and can undergo oxidation and reduction easily.

Similarly, activated carbon has a high effective surface area (typically nearly 300 to 600 m<sup>2</sup> g<sup>-1</sup>) which allows maximum ion adsorption.

Sr. No.	Type of Electrode	Synthesis	Electrolyte	Voltage	Current Density	Specific Capacitance
---------	-------------------	-----------	-------------	---------	-----------------	----------------------

				<b>Range (V)</b>		
1	3 electrode	microwave-reinforced liquid-phase	2 M KOH	-0.1 to 0.65	8 A g <sup>-1</sup>	247 mAh g <sup>-1</sup>
2	3 electrode	Simplistic Hydrothermal	2 M KOH	0 to 0.4	1 A g <sup>-1</sup>	1158 F/g
3	3 electrode	Hydrothermal	6 M KOH	0 to 0.4	5 mA cm <sup>-2</sup>	714.2 mF cm <sup>-2</sup>
4	3 electrode	In-situ	1 M KOH	0 to 1.7	4 mA cm <sup>-2</sup>	342.1 mA h g <sup>-1</sup>
5	3 electrode	Hydrothermal reaction	3 M KOH	0 to 0.5	1 A g <sup>-1</sup>	103.9 F g <sup>-1</sup>
6	3 electrode	Solvothermal	gel electrolyte (KOH-PVA)	0 to 0.4	1 A g <sup>-1</sup>	603.97 F g <sup>-1</sup>
7	3 electrode	Microwave Synthesis	2 M KOH	0 to 0.4	1 A g <sup>-1</sup>	1502 F g <sup>-1</sup>
8	3 electrode	Hydrothermal	1 M KOH	-0.1 to 0.6	0.5 A g <sup>-1</sup>	1406.9 F g <sup>-1</sup>
9	3 electrode	Electrodeposition	PVA/KOH gel electrolyte	0 to 0.5	5 mA cm <sup>-2</sup>	2.27 F cm <sup>-2</sup>
10	3 electrode	Solvothermal	2 M KOH	0 to 0.5	0.5 A g <sup>-1</sup>	2553.9 F g <sup>-1</sup>

### References:

[1] S. Rafai, C. Qiao, M. Naveed, Z. Wang, W. Younas, S. Khalid, C. Cao, *Chem. Eng. J.*, 2019, **01**, 059

[2] K. D. Ikkurthi, S. S. Rao, M. Jagadeesh, A. E. Reddy, A. Tarugu and H.J. Kim, *New J. Chem.*, 2018, **42**, 19183.

[3] J-W. Cheng, L-Y. Lin, W-L. Hong, L-Y. Lin, H-Q. Chen, H-X. Lai *Electrochimica Acta* 2018, **283**, 1245.

- [4] G. S. R. Raju, E. Pavitra, G. Nagaraju, S. ChandraSekhar, S. M. Ghoreishian, C. H. Kwak, J. S. Yu, Y. S. Huh and Y-K. Han *J. Mater. Chem. A*, 2018, **6**, 13178.
- [5] C. Chen, M. Wu, K. Tao, J. Zhou, Y. Li, X. Han and L. Han, *Dalton Trans.*, 2018, **47**, 5639.
- [6] N. Parveen, S.A. Ansari, S.G. Ansari, H. Fouad, N.M. Abd El-Salam, M.H. Cho, *Electrochimica Acta*, 2018, **01**, 100.
- [7] F. Wang, G. Li, J. Zheng, J. Ma, C. Yang, Q. Wang, *J. Colloid Interface Sci.*, 2018, **01**, 038.
- [8] K. Tao, X. Han, Q. Mab and L. Han, *Dalton Trans.*, 2018, **47**, 3496.
- [9] C. Chen, D. Yan, X. Luo, W. Gao, G. Huang, Z. Han, Y. Zeng, and Z. Zhu, *ACS Appl. Mater. Interfaces*, 2018, **10**, 4662.
- [10] D. Zhaa, Y. Fua, L. Zhangb, J. Zhua, X. Wanga, *J. Power Sources* 2018, **378**, 31.

## **Chapter 3. Experimental Section:**

### **3.1 Chemicals:**

Sodium Hydroxide(NaOH), Poly(vinylidene fluoride)(PVDF), N-methyl pyrrolidone(NMP), Carbon Black (CB), Potassium Hydroxide(KOH), Nickel Nitrate hexahydrate, Cobalt Nitrate Hexahydrate, Sodium Sulphide, Deionized water, Carbon prepared from rice husk.

### **3.2 Preparation of Nickel-Cobalt-Sulfide:**

Nickel-Cobalt-Sulfide samples have been synthesized with the help of a simplistic hydrothermal reaction. A  $\text{Co}(\text{NO}_3)_2 \cdot 6\text{H}_2\text{O}$  solution (2.5 mL) was mixed with a solution of  $\text{Ni}(\text{NO}_3)_2 \cdot 6\text{H}_2\text{O}$  at volume ratio of 1:1 at the same concentration (0.2 M) before being diluted with 50.0 mL of deionized water. A 0.1 M  $\text{Na}_2\text{S}$  solution (10.0 mL) was given drop by drop to the solution under continuous and intense stirring. The collected suspension had been transferred to a 100-mL Teflon-lined stainless steel autoclave and was given heat of 120°C for 12 h. The Ni-Co-S samples have been collected after centrifuging, washing and drying.

### **3.3 Preparation of Activated Carbon from rice husk:**

Rice husk was grounded to obtain powder and burnt at 750°C for 4 hours with increasing temperature of 3 degree per minute. After that the prepared carbon was activated by mixing with NaOH in 1:1 ratio with minimum of water (generally 2 g of carbon mixed with 2 g of NaOH in 5 mL of water) and kept stirring for overnight. It was washed with water, dried and used as active materials.

### **4.4 Fabrication of the cells**

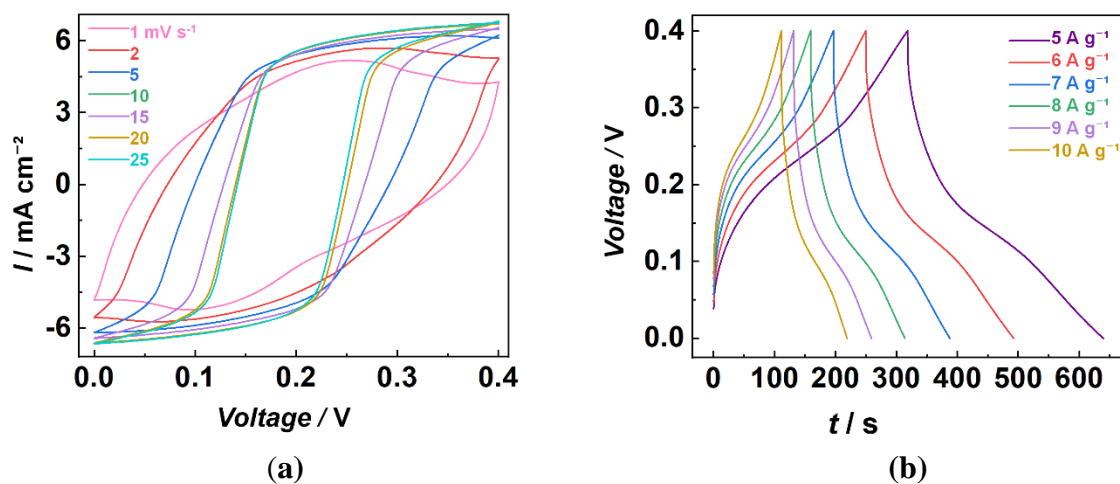
The preparation of the working electrodes (Ni-Co-S/Carbon Cloth) and carbon/carbon cloth is as follows: as prepared active materials, i.e., Ni-Co-S and activated carbon from rice husk, PVDF as a binder and carbon black were taken in a weight ratio of 60:20:10:10 respectively into the mortar pestle and grounded to get fine powder with a few drops of NMP solvent to get a slurry. Then finally slurry was applied over the carbon cloth with the use of doctor blade and dried inside the vacuum oven at 80°C for 12 h. Finally, the working electrode was collected. Similarly, another slurry was prepared with the

activated carbon from rice husk: PVDF: CB by mixing the 3 components in weight ratio of 80 :10 :10. This slurry was also applied over the carbon cloth and dried under vacuum at the same temperature overnight to obtain the Carbon (from puffed rice)/Carbon cloth electrode. 3 M KOH was being used for all electrochemical studies. The capacitive properties of the active materials have been examined with the help of cyclic voltammetry (CV) and electrochemical impedance spectroscopy (EIS) measurements. In addition, galvanostatic charge discharge (GCD) analysis also were performed. A regular three-electrode system was applied with the electrode materials coated on the carbon cloth in the form of electrode material. Platinum wire and Silver/Silver Chloride electrode have been employed as the counter electrode and reference electrode respectively.

### 3.5 Results and Discussion

#### 3.5.1 Electrochemical Properties of Ni-Co-S/Carbon cloth

Cyclic voltammetry, galvanostatic charge/discharge, and EIS electrochemical measurements studies have been executed for a symmetrical device of Ni-Co-S in a 3M KOH electrolyte. Furthermore, the Ni-Co-S/Carbon cloth electrode showed uniform CV plots as scanning rates had been enhanced from  $1 \text{ mVs}^{-1}$  to  $25 \text{ mVs}^{-1}$ . Galvanostatic charge/discharge measurements were examined by varying current densities. These studies were done in a three electrode cell, with Ag/AgCl/KCl as reference electrode and Platinum as the counter electrode.



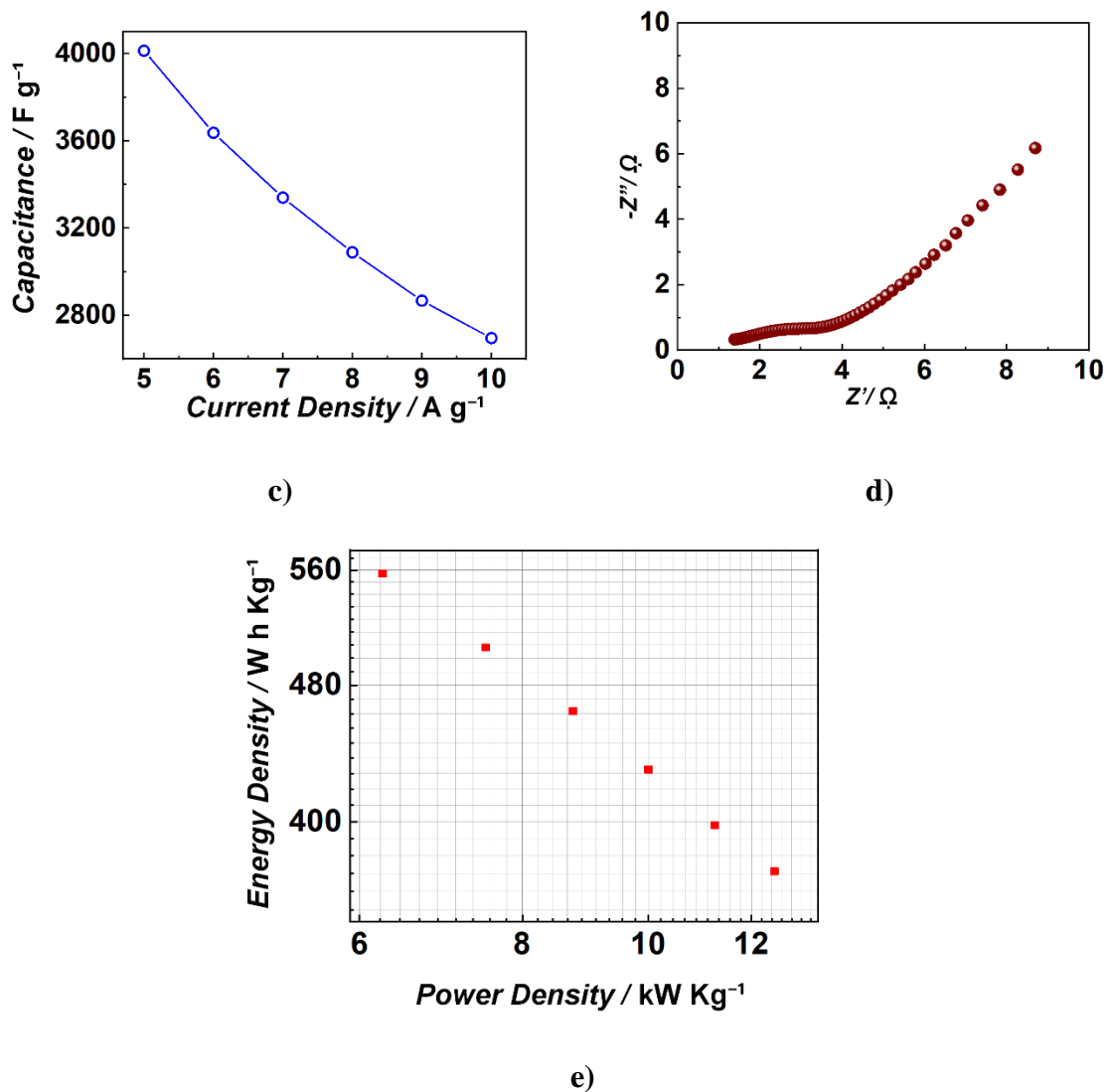


Fig. 3.5.1a) CV curves of Nickel-Cobalt-Sulfide calculated underneath varying scanning rates from 5 mVs<sup>-1</sup> to 25 mVs<sup>-1</sup> in a 3M KOH electrolyte b) Galvanostatic charge/discharge curves of Nickel-Cobalt-Sulfide low and high current density of Nickel-Cobalt-Sulfide are from 5A g<sup>-1</sup> to 10 A/cm<sup>2</sup>. c) Dependences of specific capacitance of Nickel-Cobalt-Sulfide at varying current densities from 5 A g<sup>-1</sup> to 10 A g<sup>-1</sup> for charge-discharge behaviour. d) Nyquist plot for Nickel-Cobalt-Sulfide, obtained in 3M KOH electrolyte at frequency range 0.1 Hz to 1 MHz e) Comparison of energy and power densities of Nickel-Cobalt-Sulfide/Carbon cloth SCs in a ragone plot.

**Fig. 3.5.1(a)** presents the Cyclic Voltammetry curves of the Nickel-Cobalt-Sulfide electrode in a 3.0 Molar Potassium Hydroxide solution at a scanning rate of 1 mV s<sup>-1</sup> to

25 mV s<sup>-1</sup>. The redox peaks correspond to the oxidation of metal sulphides and their contradictory reduction processes.

**Fig. 3.5.1(b)** presents the charge discharge curves of the Nickel-Cobalt-Sulfide electrode underneath variety of current densities (5-10 A g<sup>-1</sup>).

The specific capacitance has been evaluated from the charge/discharge curves according to the following equation

$$C = I(\Delta t) / m(\Delta V)$$

Where I designates the discharge current,  $\Delta t$  designates the discharge time, m is the total mass of the material, and  $\Delta V$  designates the functioning voltage after iR drop. The evaluated specific capacitances are plotted in **Fig. 3.5.1(c)** (plot capacitance vs current density). The maximum specific capacitance (4000 F/cm<sup>2</sup>) of Nickel-Cobalt-Sulfide/Carbon cloth electrode was obtained at 5 mA/cm<sup>2</sup>. The capacitances of the Nickel-Cobalt-Sulfide electrode at 5, 6, 7, 8, 9 and 10 mA/cm<sup>2</sup> are 4012.5, 3636, 3339, 3088, 2866.5 and 2695 F/cm<sup>2</sup> respectively.

**Fig.3.5.1(d)** shows the Nyquist plots collected from EIS measurements over the frequency ranging from 10 mHz to 1 MHz.

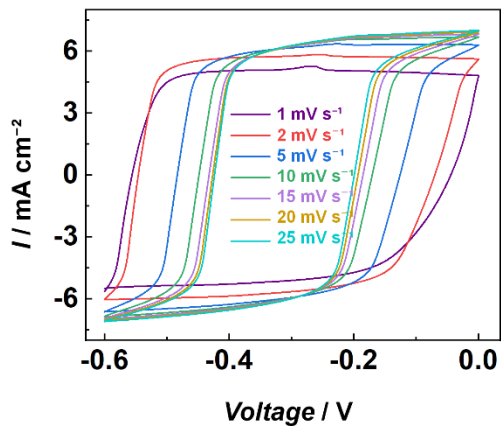
Energy and power densities of the SCs have been evaluated and plotted with the help of galvanostatic charge/discharge test results (**Fig. 3.5.1 (e)**). The SCs showed an energy density of 560 W h Kg<sup>-1</sup> at a power density of 6100 W Kg<sup>-1</sup>.



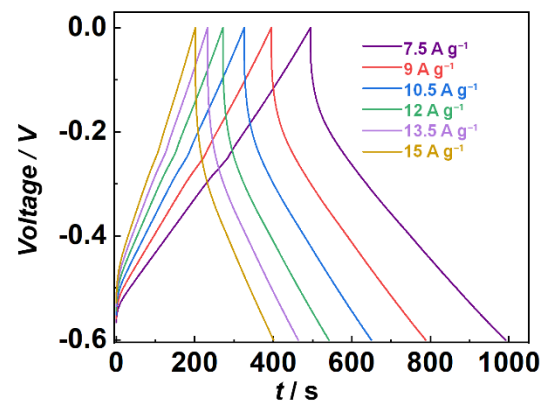
**Table 3: Brief description of charge discharge, specific capacitance, energy density and power density of Ni-Co-S.**

Sr. No.	Current Density(A g <sup>-1</sup> )	Capacitance (F g <sup>-1</sup> )	Energy Density(W h Kg <sup>-1</sup> )	Power Density(kW Kg <sup>-1</sup> )
1.	5	4012.5	557	6250
2.	6	3636	505	7500
3.	7	3339	463.75	8750
4.	8	3088	429	10000
5.	9	2866.5	398	11250
6.	10	2695	374	12500

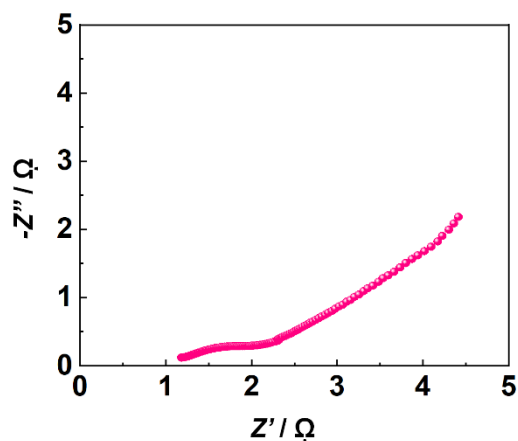
### 3.5.2. Electrochemical Properties of activated Carbon/Carbon cloth:



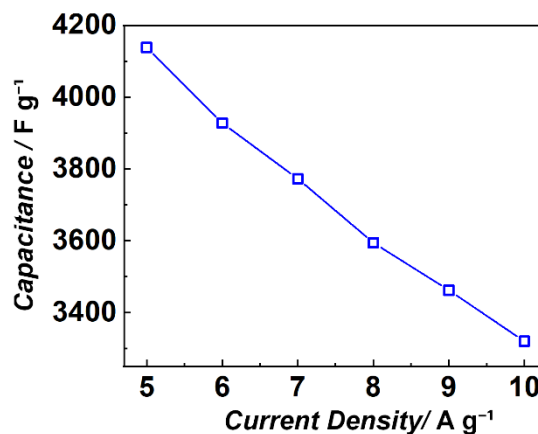
a)



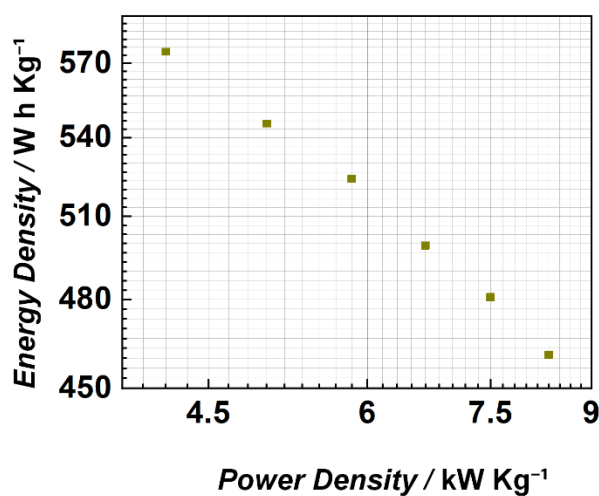
b)



c)



d)



e)

Fig. 3.5.2a) CV curves of Carbon calculated at the varying scan rates from  $1\text{mVs}^{-1}$  to  $25\text{mVs}^{-1}$  in a  $3\text{M KOH}$  electrolyte, b) Galvanostatic charge/discharge curves of Carbon low and high current density of Carbon are from  $5\text{ A g}^{-1}$  to  $10\text{ A g}^{-1}$ . c) Dependences of specific capacitance of Carbon at variety of current densities from  $5\text{ A g}^{-1}$  to  $10\text{ A g}^{-1}$  for charge-discharge behaviour. d) Nyquist plot for Carbon, obtained in  $3\text{M KOH}$  electrolyte at frequency range  $0.1\text{ Hz}$  to  $1\text{ MHz}$  e) Contrast between energy and power densities of Activated Carbon (from rice husk)/Carbon cloth SCs.

**Fig. 3.5.2(a)** presents the Cyclic Voltammetry curves of the Activated Carbon (from rice husk)/Carbon cloth electrode in a 3.0 Molar Potassium Hydroxide solution at a scanning rate of 1 mV s<sup>-1</sup> to 25 mV s<sup>-1</sup>. The redox peaks correspond to the oxidation of metal sulphides and their contradictory reduction processes.

**Fig. 3.5.2(b)** provides the charge discharge curves of the Activated Carbon (from rice husk)/Carbon cloth electrode at different current densities (7.5,9,10.5,12,13.5,15 A g<sup>-1</sup>). The specific capacitance was evaluated from the charge/discharge curves according to the following equation

$$C=I(\Delta t)/m(\Delta V)$$

The evaluated specific capacitances are plotted in **Fig. 3.5.2(c)** (plot capacitance vs current density). The highest specific capacitance (4180 F g<sup>-1</sup>) of Activated Carbon (from rice husk)/Carbon cloth electrode was obtained at 5 mA g<sup>-1</sup>. The capacitances of the Carbon (from puffed rice)/Carbon cloth electrode at 5, 6, 7, 8, 9 and 10 mA g<sup>-1</sup> are 4138.33, 3928, 3773, 3594.6, 3462 and 3320 F g<sup>-1</sup> respectively.

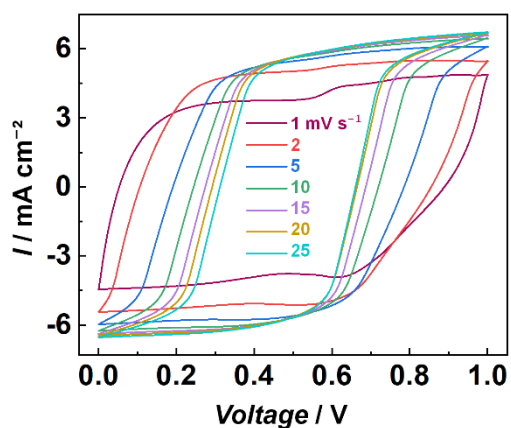
**Fig. 3.5.2(d)** shows the Nyquist plots collected from EIS measurements over the frequency ranging from 10mHz to 1 MHz. The introductory resistance results from the solution resistance which is almost equal to 1.1 Ω. However, the Charge transfer resistance (R<sub>ct</sub>) is nearly 2.49 Ω.

Energy and power densities of the SCs have been evaluated and plotted with the help of galvanostatic charge/discharge test results (**Fig. 3.5.2 (e)**). The SCs showed an energy density of 570 W h kg<sup>-1</sup> at a power density of 420 W kg<sup>-1</sup>.

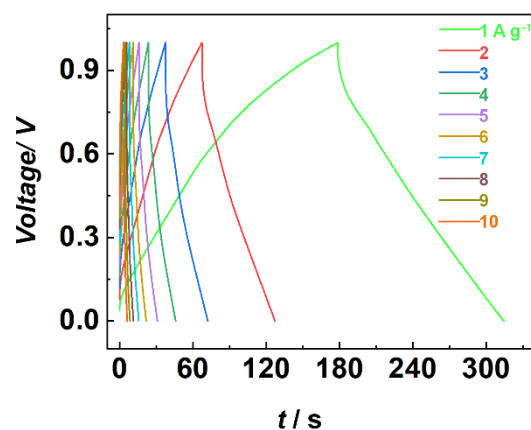
**Table 4: Brief description of charge discharge, specific capacitance, energy density and power density of Activated Carbon.**

<b>Sr. No.</b>	<b>Current Density (A g<sup>-1</sup>)</b>	<b>Capacitance (F g<sup>-1</sup>)</b>	<b>Energy Density (W h Kg<sup>-1</sup>)</b>	<b>Power Density (kW Kg<sup>-1</sup>)</b>
1.	5	4138.33	575	4167
2.	6	3928	546	5000
3.	7	3773	524	5833
4.	8	3594.6	499	6667
5.	9	3462	481	7500
6.	10	3320	461	8333

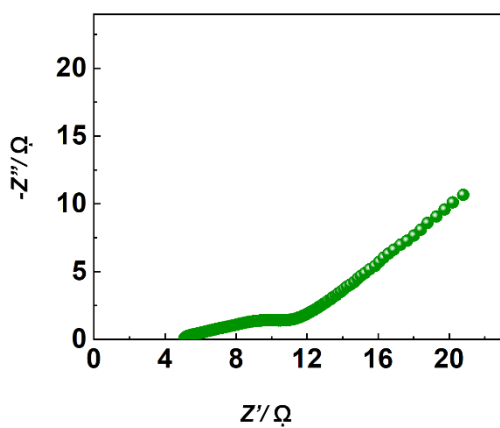
### 3.5.3. Electrochemical Properties of Ni-Co-S//Activated Carbon:



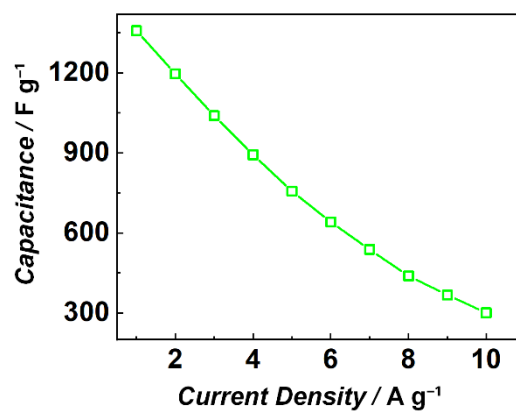
a)



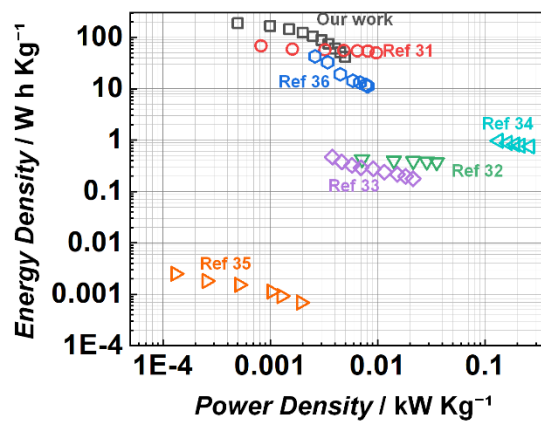
b)



c)



d)



e)

Fig. 3.5.3a) CV curves of Cell calculated at the varying scan rates at 1, 2, 5, 10, 15, 20, 25  $\text{mVs}^{-1}$  in a 3M KOH electrolyte, b) Galvanostatic charge/discharge curves of Cell low and high current density of Cell are from 1  $\text{A g}^{-1}$  to 10  $\text{A g}^{-1}$ . c) Dependences of specific capacitance of Cell at variety of the current densities from 1  $\text{A g}^{-1}$  to 10  $\text{A g}^{-1}$  for charge-discharge behaviour. d) Nyquist plot for Cell, obtained in 3M KOH electrolyte at frequency range 0.1 Hz to 1 MHz e) Comparison of energy and power densities of Cell in a Ragone plot.

**Fig. 3.5.3(a)** presents the Cyclic Voltammetry curves of the Nickel-Cobalt-Sulfide/Carbon in a 3.0 Molar Potassium Hydroxide solution at a scan rate of 1, 2, 5, 10, 15, 20, 25  $\text{mV s}^{-1}$ . The redox peaks correspond to the oxidation of metal sulphides and their contradictory reduction processes.

**Fig. 3.5.3(b)** shows the charge discharge curves of the Activated Carbon (from rice husk)/Carbon cloth electrode underneath variety of current densities (1, 2, 3, 4, 5, 6, 7, 8, 9, 10  $\text{A g}^{-1}$ ).

The specific capacitance has been evaluated from the charge/discharge curves according to the following equation

$$C = \frac{I(\Delta t)}{m(\Delta V)}$$

The evaluated specific capacitances are plotted in **Fig. 3.5.3(c)** (plot capacitance vs current density). The maximum specific capacitance ( $1358.2 \text{ F g}^{-1}$ ) of Ni-Co-S/Carbon (from puffed rice) electrode was obtained at 1  $\text{mA g}^{-1}$ . The capacitances of the Ni-Co-S/Carbon (from rice husk) electrode at 1, 2, 3, 4, 5, 6, 7, 8, 9 and 10  $\text{mA g}^{-1}$  are 1358.2, 1196.4, 1039.2, 892.8, 756, 640.8, 537.6, 438.4, 367.2, 300  $\text{F g}^{-1}$  respectively.

**Fig. 3.5.3(d)** shows the Nyquist plots obtained from EIS measurements over the frequency ranging from 10 mHz to 1 MHz. A semicircular loop at higher frequencies is observed as a result of the charge-transfer resistance ( $R_{ct}$ ), which corresponds to the resistance of the electrochemical reaction on the electrode and is called the Faraday resistance. Introductory resistance appears from solution resistance ( $R_S$ ). It is almost equal to 5.7  $\Omega$ . However, the Charge transfer resistance is nearly 11.9  $\Omega$ .

Energy and power densities of the SCs have been evaluated and plotted with the help of galvanostatic charge/discharge test results (**Fig. 3.5.3 (e)**). It correlates Ragone plots of Nickel-Cobalt-Sulfide//Carbon hybrid supercapacitor with those of many other relevant works. It showed an energy density of  $190 \text{ W h kg}^{-1}$  at a power density of  $500 \text{ W kg}^{-1}$ . For example, Chen *et al* reported positive electrode component for hybrid supercapacitor,  $\text{CoNi}_2\text{S}_4$  nanosheets established exceptional electrochemical performances and provides a highest energy density of  $67.7 \text{ Wh kg}^{-1}$  at a power density of  $0.8 \text{ kW kg}^{-1}$  [31], Hee-Je *et al* reported a coral reef-like nanostructure of NiS/NF, synthesized so that it can be used in SCs by simplistic hydrothermal mechanism with higher energy density of  $54.88 \text{ W h kg}^{-1}$  at a power density of  $500 \text{ W kg}^{-1}$  [32], Cheng *et al* reported the rational-designed core/shell structures by first developing the Ni-Co-S nanosheet array on the Ni foam with the use of a hydrothermal mechanism as the core, (which gives enormous energy density of  $0.43 \text{ W h kg}^{-1}$ ) was accomplished at the power density of  $7.17 \text{ W kg}^{-1}$  [33], Young *et al* proclaimed three-dimensional forest-like porous nickel sulfide nanotrees on nickel foam (NiS NTs/Ni foam), which provides high areal energy and power densities of  $0.472 \text{ mW h cm}^{-2}$  and  $21.5 \text{ mW cm}^{-2}$ , respectively [34], Chen *et al* proclaimed the asymmetric supercapacitor device together with Nickel-Cobalt-Sulfide provides a maximum energy density of  $36.9 \text{ W h kg}^{-1}$  at a power density of  $1066.42 \text{ W kg}^{-1}$  and good cycling stability of 83.01% [35], Hwan Cho *et al* proclaimed mesoporous nickel sulfide (NiS) stratified framework prepared with the help of a simplistic solvothermal method and it also provides maximum energy of  $0.2477 \text{ W h kg}^{-1}$  at a power density of  $33.24 \text{ W Kg}^{-1}$

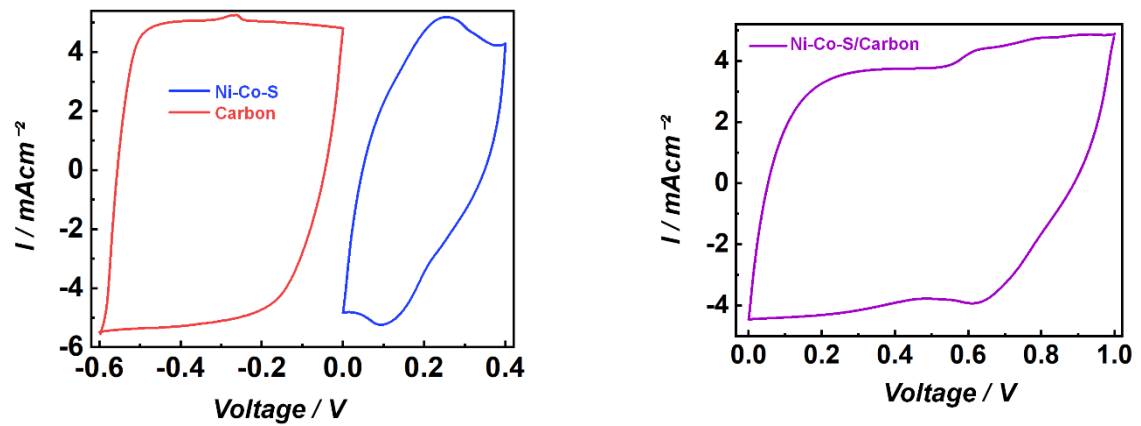
**Table 5: Brief description of charge discharge, specific capacitance, energy density and power density of Nickel-Cobalt-Sulfide//Activated Carbon electrode.**

Sr. No.	Current Density (A g <sup>-1</sup> )	Capacitance (F g <sup>-1</sup> )	Energy Density (W h Kg <sup>-1</sup> )	Power Density (kW Kg <sup>-1</sup> )
1.	1	1358.2	189	500
2.	2	1196.4	166	1000
3.	3	1039.2	144	1500
4.	4	892.8	124	2000
5.	5	756	105	2500
6.	6	640.8	89	3000
7.	7	537.6	75	3500
8.	8	438.4	61	4000
9.	9	367.2	51	4500
10.	10	300	42	5000



## Chapter 4:

Comparison between CV of Nickel-Cobalt-Sulfide, Carbon and Nickel-Cobalt-Sulfide//Activated Carbon electrodes at  $1\text{ mV s}^{-1}$



These plots show that Ni-Co-S stores and releases charge as a cathode and Activated carbon can act as an anode.

**Conclusions:**

In summary, nickel-cobalt-sulfides were synthesized with the help of a simple hydrothermal mechanism. The Nickel-Cobalt-Sulfide/Carbon cloth electrode displays a maximum specific capacitance of  $4000 \text{ F cm}^{-2}$ . In addition, the energy density of the Nickel-Cobalt-Sulfide//Activated Carbon based asymmetric supercapacitor is  $190 \text{ W h Kg}^{-1}$  at a power density of  $500 \text{ kW Kg}^{-1}$ . On the basis of these conclusions, the Nickel-Cobalt-Sulfide//Activated Carbon electrode material has acceptable potential for application as asymmetric supercapacitor.

## REFERENCES

- [1] R. B. Pujari, A. C. Lokhande, A. R. Shelke, J. H. Kim and C. D. Lokhande, J. *Colloid Interface Sci.*, 2017, **496**, 1.
- [2] B. Pandit, D. P. Dubal, P. Go´mez-Romero, B. B. Kale and B. R. Sankapal, *Sci. Rep.*, 2017, **7**, 43430.
- [3] L. Hao, L. Shen, J. Wang, Y. Xu, X. Zhang, *RSC Adv.*, 2016, **6**, 9950
- [4] J. Yu, H. Wan, J. Jiang, Y. Ruan, L. Miao, L. Zhang, D. Xia and K. Xu, *J. Electrochem. Soc.*, 2014, **161**, 996.
- [5] R. R. Salunkhe, J. Tang, Y. Kamachi, T. Nakato, J. H. Kim, Y. Yamauchi, *ACS Nano*, 2015, **9**, 6288
- [6] R. Raccichini, A. Varzi, S. Passerini, B. Scrosati, *Nature Mater.*, 2015, **14**, 271.
- [7] Z. Yan, C. Min and W. Limin, *Nanotechnology*, 2016, **27**, 342001
- [8] Z. Yang, J. Ren, Z. Zhang, X. Chen, G. Guan, L. Qiu, Y. Zhang and H. Peng, *Chem. Rev.*, 2015, **115**, 5159.
- [9] Y. Tang, Y. Liu, S. Yu, Y. Zhao, S. Mu, F. Gao, *Electrochim. Acta* ,2014 ,**123**, 158.
- [10] A. Wang, H. Wang, S. Zhang, C. Mao, J. Song, H. Niu, B. Jin, Y. Tian, *Appl. Surf. Sci.*, 2013, **273**, 704.

- [11] J. Miot, N. Recham, D. Larcher, F. Guyot, J. Brest, J. M. Tarascon, *Energy Environ. Sci.* 2014, **7**, 451.
- [12] S. W. Chou, J. Y. J. Lin, *Electrochem. Soc.* 2013, **160**, 187.
- [13] T. Peng, Z. Qian, J. Wang, D. Song, J. Liu, Q. Liu, P. Wang, *J. Mater. Chem. A*, 2014, **2**, 19376
- [14] Zhu, T.; Wu, H. B.; Wang, Y. B.; Xu, R.; Lou, X. W. *Adv. Energy Mater.* 2012, **2**, 1497.
- [15] W. Shi, J. Zhu, X. Rui, X. Cao, C. Chen, H. Zhang, H. H. Hng, Q. Yan, *ACS Appl. Mater. Interfaces*, 2012, **4**, 2999.
- [16] D. Vernardou, A. Sapountzis, E. Spanakis, G. Kenanakis, E. Koudoumas, N. Katsaraki, *J. Electrochem. Soc.*, 2013, 160, 6.
- [17] M. Li, G. Sun, P. Yin, C. Ruan, K. Ai, *Appl. Mater. Interf.*, 2013, **5**, 11462.
- [18] Q. Pan, J. Xie, S. Liu, G. Cao, T. Zhu, X. Zhao, *RSC Advances*, 2013, **3**, 3899.
- [19] B. Wang, J. Park, D. Su, C. Wang, H. Ahn, G. Wang, *J. Mater. Chem.*, 2012, **12**, 15750.
- [20] W. Kong, C. Lu, W. Zhang, J. Pu, Z. Wang, *J. Mater. Chem. A*, 2015, **3**, 12452.
- [21] L. Jin, B. Liu, Y. Wu, S. Thanneeru, J. He, *ACS Appl. Mater. Interfaces*, 2017, **9**, 36837
- [22] Y. Wang, Y. Song, Y. Xia, *Chem. Soc. Rev.* 2016, **45**, 5925.

- [23] Z. J. Han, S. Pineda, A. T. Murdock, D. H. Seo, K. Ostrikov and A. Bendavid, *J. Mater. Chem. A*, 2017, **5**, 17293.
- [24] S. S. Rao, I. K. Durga, N. Kundakarla, D. Punnoose, C. V. V. M. Gopi, A. E. Reddy, M. Jagadeesh and H. J. Kim, *New J. Chem.*, 2017, **41**, 10037.
- [25] A. Kumar, A. Sanger, A. Kumar, Y. K. Mishra and R. Chandra, *Chemistry Select*, 2016, **1**, 3885.
- [26] A. V. Radhamani, K. M. Shareef and M. S. R. Rao, *ACS Appl. Mater. Interfaces*, 2016, **8**, 30531.
- [27] W. Li, S. Wang, L. Xin, M. Wu and X. Lou, *J. Mater. Chem. A*, 2016, **4**, 7700.
- [28] T. Lv, Y. Yao, N. Li and T. Chen, *Angew. Chem., Int. Ed.*, 2016, **55**, 9191.
- [29] N. Li, T. Lv, Y. Yao, H. Li, K. Liu and T. Chen, *J. Mater. Chem. A*, 2017, **5**, 3267.
- [30] S. Sahoo, R. Mondal, D. J. Late and C. S. Rout, *Microporous Mesoporous Mater.*, 2017, **244**, 101.
- [31] S. Rafai, C. Qiao, M. Naveed, Z. Wang, W. Younas, S. Khalid, C. Cao, *Chem. Eng. J.*, 2019, **01**, 059
- [32] K. D. Ikkurthi, S. S. Rao, M. Jagadeesh, A. E. Reddy, A. Tarugu and H.J. Kim, *New J. Chem.*, 2018, **42**, 19183.
- [33] J-W. Cheng, L-Y. Lin, W-L. Hong, L-Y. Lin, H-Q. Chen, H-X. Lai, *Electrochimica Acta* 2018, **283**, 1245.

- [34] G. S. R. Raju, E. Pavitra, G. Nagaraju, S. ChandraSekhar, S. M. Ghoreishian, C. H. Kwak, J. S. Yu, Y. S. Huh and Y-K. Han, *J. Mater. Chem. A*, 2018, **6**, 13178.
- [35] C. Chen, M. Wu, K. Tao, J. Zhou, Y. Li, X. Han and L. Han, *Dalton Trans.*, 2018, **47**, 5639.
- [36] N. Parveen, S.A. Ansari, S.G. Ansari, H. Fouad, N.M. Abd El-Salam, M.H. Cho, *Electrochimica Acta*, 2018, **01**, 100.
- [37] F. Wang, G. Li, J. Zheng, J. Ma, C. Yang, Q. Wang, *J. Colloid Interface Sci.*, 2018, **01**, 038.
- [38] K. Tao, X. Han, Q. Mab and L. Han, *Dalton Trans.*, 2018, **47**, 3496.
- [39] C. Chen, D. Yan, X. Luo, W. Gao, G. Huang, Z. Han, Y. Zeng, and Z. Zhu, *ACS Appl. Mater. Interfaces*, 2018, **10**, 4662.
- [40] D. Zhaa, Y. Fua, L. Zhangb, J. Zhua, X. Wang, *J. Power Sources* 2018, **378**, 31.
- [41] S. Xu, C. Su, T. Wang, Y. Ma, J. Hu, J. Hu, N. Hu, Y. Su, Y. Zhang, Z. Yang, *Electrochim. Acta*, 2017, **11**, 027.
- [42] L. Jin, B. Liu, Y. Wu, S. Thanneeru, and J. He, *ACS Appl. Mater. Interfaces*, **42**, 36837
- [43] K. Krishnamoorthy, G. K. Veerasubramani, S. Radhakrishnan, S. J. Kim, *Chem. Eng. J.*, 2014, **251**, 116.
- [44] U. M. Patil, P. K. Katkar, S. J. Marje, C. D. Lokhandea and S. C. Jun, *New J. Chem.*, 2018, **42**, 20123.

[45] W. li, S. Wang, L. Xin, M. Wu and X. Lou, *J. Mater. Chem. A*, 2016, **20**, 7700.